EPIGENETICS
2025, VOL. 20, NO. 1, 2473770
https://doi.org/10.1080/15592294.2025.2473770

Taylor & Francis
Taylor & Francis Group

RESEARCH ARTICLE

OPEN ACCESS Check for updates

SIRT1/DNMT3B-mediated epigenetic gene silencing in response to phytoestrogens in mammary epithelial cells

Yuexi Ma, Cayla Boycott, Jiaxi Zhang, Rekha Gomilar, Tony Yang, and Barbara Stefanska

Food, Nutrition and Health Program, Faculty of Land and Food Systems, The University of British Columbia, Vancouver, BC, Canada

ABSTRACT

We performed an integrated analysis of genome-wide DNA methylation and expression datasets in normal cells and healthy animals exposed to polyphenols with estrogenic activity (i.e. phytoestrogens). We identified that phytoestrogens target genes linked to disrupted cellular homeostasis, e.g. genes limiting DNA break repair (*RNF169*) or promoting ribosomal biogenesis (*rDNA*). Existing evidence suggests that DNA methylation may be governed by sirtuin 1 (SIRT1) deacetylase via interactions with DNA methylating enzymes, specifically DNMT3B. Since SIRT1 was reported to be regulated by phytoestrogens, we test whether phytoestrogens suppress genes related to disrupted homeostasis via SIRT1/DNMT3B-mediated transcriptional silencing. Human MCF10A mammary epithelial cells were treated with phytoestrogens, pterostilbene (PTS) or genistein (GEN), followed by analysis of cell growth, DNA methylation, gene expression, and SIRT1/DNMT3B binding. SIRT1 occupancy at the selected phytoestrogen-target genes, *RNF169* and *rDNA*, was accompanied by consistent promoter hypermethylation and gene downregulation in response to GEN, but not PTS. GEN-mediated hypermethylation and SIRT1 binding were linked to a robust DNMT3B enrichment at *RNF169* and *rDNA* promoters. This was not observed in cells exposed to PTS, suggesting a distinct mechanism of action. Although both SIRT1 and DNMT3B bind to *RNF169* and *rDNA* promoters upon GEN, the two proteins do not co-occupy the regions. Depletion of SIRT1 abolishes GEN-mediated decrease in *rDNA* expression, suggesting SIRT1-dependent epigenetic suppression of *rDNA* by GEN. These findings enhance our understanding of the role of SIRT1-DNMT3B interplay in epigenetic mechanisms mediating the impact of phytoestrogens on cell biology and cellular homeostasis.

ARTICLE HISTORY
Received 29 October 2024
Revised 20 February 2025
Accepted 24 February 2025

KEYWORDS
SIRT1; DNMT3B; epigenetic gene silencing; protein-DNA interaction; mammary epithelial cells

Introduction

Epigenetics refers to the regulation of gene expression without changes in the underlying DNA sequence. It comprises several components, including DNA methylation, histone covalent modifications, non-coding RNA mechanisms, and chromatin remodeling complexes [1]. Epigenetic control of gene expression is at the forefront of cellular homeostasis via regulation of almost every biological process, thereby maintaining health, decelerating aging, and preventing disease [2]. Among epigenetic components, DNA methylation at gene regulatory regions is associated with transcriptional silencing [3], and is believed to provide stable and long-term regulation of gene expression [4]. Furthermore, DNA methylation strongly engages in a crosstalk with other epigenetic mechanisms, including histone covalent modifications [5]. DNA methyltransferases (DNMTs), that are DNA methylating enzymes, directly interact with histone modifications and with enzymes involved in modifying histone tails, including histone deacetylases (HDACs) [4–8]. Histones deacetylated by HDACs exhibit stronger electrostatic interactions with DNA, leading to compacted chromatin and reduced transcriptional activity [9]. Recent studies show the interplay between histone deacetylase SIRT1 and *de novo* DNA methyltransferase DNMT3B in the context of restricting proinflammatory gene activation [7]. SIRT1 was also shown to recruit DNMT3B to SIRT1-associated chromatin for subsequent DNA methylation and chromatin condensation [8], which was observed in transcriptional silencing required for DNA damage repair [10]. SIRT1 belongs to a family of nicotinamide adenosine dinucleotide (NAD)-

CONTACT Barbara Stefanska barbara.stefanska@ubc.ca Food, Nutrition and Health Program, Faculty of Land and Food Systems, The University of British Columbia, 2205 East Mall, FNH 150, Vancouver, BC V6T 1Z4, Canada

Supplemental data for this article can be accessed online at https://doi.org/10.1080/15592294.2025.2473770

dependent deacetylases that remove acetyl groups from both histone and non-histone proteins [11]. Through acting as a histone deacetylase, SIRT1 regulates chromatin structure and impacts gene expression. Deacetylation of epigenetic regulators, such as DNMT1, p300, and SUV39H1, constitutes an additional mechanism of SIRT1-mediated regulation of chromatin condensation [12]. Multiple functions of SIRT1 are also exerted through deacetylation of transcription factors, e.g., deacetylation of FOXO family of transcription factors enhances their activity in antioxidant processes, apoptosis, and cell proliferation [13], deacetylation of the p65 subunit of NF-κB complex inhibits NF-κB signaling and the inflammatory response [14], and deacetylation of a transcription coactivator, PGC-1α, regulates energy homeostasis [15]. Furthermore, SIRT1 exerts additional actions via a deacetylase-independent mechanism and regulates signaling pathways. For instance, recent findings show SIRT1 as an activator of the PI3K/AKT/FOXO1 signaling pathway which is correlated with increased angiogenesis and vascular regeneration during bone repair [16].

Of interest, SIRT1 expression/activity has been shown to be regulated by naturally occurring dietary polyphenols, including compounds from a group of phytoestrogens [17]. Phytoestrogens offer pro-longevity and pro-health benefits in a variety of different disease models, including metabolic syndrome, type 2 diabetes, cardiovascular disease, and cancer [18]. One of the most studied phytoestrogens, resveratrol (RSV), was the first to be shown to activate SIRT1 and enhance SIRT1-dependent cellular processes in yeast [19]. Although a direct interaction between RSV and SIRT1 was later challenged [20], changes in SIRT1 in response to RSV have been widely reported [21]. RSV analog, pterostilbene (PTS) from blueberries, has also been shown to act, at least partially, via SIRT1. Compared to RSV, PTS is characterized by greater bioavailability, hepatic stability, and bioactivity [22]. Therefore, PTS is a compound of interest for further investigation. Previous research has shown enhanced SIRT1 expression in response to PTS to be crucial in inhibiting oxidative stress and abnormal mitochondrial morphologies induced by acute doxorubicin exposure in cardiomyocytes [23]. Likewise, PTS-mediated SIRT1 activation was linked to increased mitochondrial biogenesis and thermogenesis, which resulted in body weight reduction in rats with western diet-induced obesity [24]. PTS has also been shown to improve neuroplasticity and reduce neuronal inflammation by increasing expression of SIRT1 and anti-inflammatory NRF2 [25,26]. Another phytoestrogen with well-studied health effects, genistein (GEN) from soy beans, has been demonstrated to regulate SIRT1 as well. SIRT1 is mechanistically involved in GEN-mediated suppression of the accumulation of lipid droplets in hepatocytes [27]. SIRT1 upregulation also accompanied GEN-mediated amelioration of liver [28] and renal injury [29]. The upregulated expression and activity of SIRT1 in association to GEN treatment was also shown to contribute to attenuation of hepatic fibrosis by downregulation of fibrosis-associated genes [30].

Studies by our group and others have shown that phytoestrogens, specifically PTS and GEN, exert epigenetic effects and remodel DNA methylation patterns [31–37]. In breast cancer cells, we showed that PTS led to the activation of methylation-silenced tumor suppressor genes, which was accompanied by a decrease in DNMT3A binding [31]. In another study, exposure to PTS resulted in hypomethylation and reactivation of ERα, sensitizing breast cancer cells to hormone therapy [32]. Epigenetic activation of tumor suppressor genes was also observed in response to GEN [33–37]. In prostate cancer, for instance, treatment with GEN induced genome-wide differential DNA methylation changes and reversed hypermethylation and silencing of BTG3 tumor suppressor [33,34]. Interestingly, apart from epigenetic reactivation of tumor suppressor genes, treatment with PTS has also resulted in increased DNA methylation within regulatory regions of key oncogenes, such as *PRKCA* in breast cancer cells [38,39]. Using CRISPR-Cas9 technology, we provided evidence that DNMT3B is required for PTS-mediated epigenetic suppression of oncogenes [38]. Although it remains unknown whether GEN alters binding of DNMT3B to DNA, its influence on DNMT3B expression and activity was previously reported [40].

Although both SIRT1 and DNMT3B have been demonstrated to be implicated in phytoestrogens' effects, there are no data on the interplay between these two epigenetic enzymes in phytoestrogens' biological action. Considering recent reports on the interaction between SIRT1 and DNMT3B, in the present study, we investigated whether SIRT1-DNMT3B interplay is involved in phytoestrogen-mediated epigenetic regulation of gene expression. The implication of SIRT1 in phytoestrogens' health-promoting effects has been shown in various disease models [17,18], but studies in normal models are largely missing. The same applies to epigenetic effects of phytoestrogens, which are mostly investigated in disease, while scarce literature in health or in normal experimental models exist [41]. Therefore, we used MCF10A cell line in our current mechanistic investigation as a well-characterized model of human mammary epithelial cells, which are non-transformed and exhibit molecular and cellular properties of normal breast epithelium [42,43]. These features enable us to study the epigenetic regulation of gene expression in maintaining/promoting cellular homeostasis. Importantly, the widespread use of MCF10A cells in biomedical research increases the significance of our study by providing knowledge that can be applied in other settings.

Materials and methods

Genome-wide data analysis and selection of phytoestrogen-target genes

Genes listed in Table 1 were selected from genome-wide data obtained from two existing datasets in normal experimental models in our laboratory. The first dataset originated from the Infinium HumanMethylation 450K BeadChip DNA methylation analysis of MCF10A control cells (treated with vehicle-ethanol) and MCF10A cells cultured with a PTS analog, namely 15 μM RSV, for 9 days ($n = 3$/condition; GEO accession number GSE113299). The second dataset involves gene expression analyzed through RNA sequencing in blood of healthy Fischer-344 rats exposed for 3 weeks to a choline-sufficient amino acid defined (CSAA) diet supplemented with PTS (1.34 g/kg of diet, between 5–8 weeks of age), compared to healthy rats fed with CSAA diet ($n = 5$ animals/group; GEO accession number GSE278528).

In the two datasets, 100 top differentially methylated genes with the highest magnitude of change and the top 53 differentially expressed genes with at least 3-fold change in expression were selected for a detailed functional analysis of each gene individually, using Gene Cards database and existing literature in PubMed. Among differentially expressed genes with $2 \leq$ fold change < 3, additional targets were selected if

Table 1. Putative phytoestrogen-target genes that are differentially methylated or expressed in normal experimental models.

Cellular homeostasis and health maintenance		
Specific function	Hypermethylated/ downregulated genes	Hypomethylated/ upregulated genes
Regulation of inflammatory response and decreased oxidative stress	GSTT1, Gstp1, Hbe1, Rnf114	AGTPBP1, PELI1, GULP1, PDCD6IP, MAP3K8, DHX15, CSF1R, CELSR2, Spef2
Cell survival and healing	FAM19A4	FGFR1OP2, MMP13, Spef2
Increased mitochondrial biogenesis and autophagy	DAO, Rnf5	RALA
Genomic stability	RNF169, Rnf114	OXR1
Reduced transformation	RTKN, KCNJ4, RNF169, GSTT1, Gstp1	ISPD, SFTA2, GULP1, EBF3, HOXA9
Regulation of DNA repair	RNF169, Rnf114	PELI1, CECR2
Proteostasis	rDNA, Rps16, ZNF625, RNF169, FBXO32, Rnf5, Rnf114	ANKIB1, Rn5s
Cell division, motility, shape and cellular transport	TUBB4, KCNJ4, SDCBP2, DYNLRB2, Slc7a5	RALA, SLC45A4, CSF1R, ORC4L, Myo15a, Megf10
Regulation of immune functions	ITGAM, HLA-DQB1, EBF4, OVOL1, Bst2, Cd52, Rnf114, Rnf5	TAGAP, EBF3, MAP3K8, DHX15, CSF1R, BCL6, Megf10
Transcription regulation and chromatin remodeling	ZNF625, ZNF155, BHMT2, TSPYL2, CBFA2T3	ZNF654, EBF3, KDM1A, SUDS3, CECR2, BCL6, TTF2, Sgsm1
Energy homeostasis	HDC	EHBP1, BAI3, ALK

The genes are implicated in processes that regulate health maintenance and cellular homeostasis.

they belonged to the same family of genes as one of the 100 top differentially methylated genes (integration of the two datasets). A descriptive summary of functions of the selected phytoestrogen-target genes is depicted in Table 1 where genes were grouped based on shared functions.

Cell culture and treatment with pterostilbene (PTS) and genistein (GEN)

The MCF10A human mammary epithelial cell line was obtained from ATCC (CRL-10317, USA). MCF10A cells were cultured in DMEM/F12 (1:1) medium (Gibco), supplemented with 20 ng/ml epidermal growth factor (Sigma-Aldrich, St. Louis, MO, USA), 100 ng/ml cholera toxin (Calbiochem, EMD Millipore, Billerica, MA, USA), 0.01 mg/ml insulin (Sigma-Aldrich, St. Louis, MO, USA), 500 ng/ml hydrocortisone (Sigma-Aldrich, St. Louis, MO, USA), 5% horse serum (Gibco), and 1 U/ml penicillin and 1 µg/ml streptomycin (Gibco). Pterostilbene (PTS) and genistein (GEN) (Cayman Chemical Company, Michigan, USA) were resuspended in ethanol and DMSO, respectively, to create a 50 mm stock solution. Dilutions of each compound were freshly prepared before each treatment. Cell cultures were maintained in a 37°C incubator and humidified atmosphere of 5% carbon dioxide. Cells were seeded at a density of 4 × 10^5 cells in 10-cm tissue culture dish and allowed to attach for 24 hours before adding media containing PTS or GEN. A range of PTS (0 to 20 µM) and GEN (0 to 40 µM) concentrations were applied. After 4 days of incubation, cells were split in a ratio of 1:50 and allowed to attach overnight followed by exposure to PTS or GEN for an additional 4 days (total 9 days).

Trypan blue exclusion test

Cell viability was assessed using the trypan blue exclusion test (Sigma-Aldrich). Cells were collected after exposure to PTS or GEN on both day 4 and day 9, as well as upon treatment with siRNAs. After a 3–5-minute incubation with trypan blue, viable and dead cells were enumerated under a microscope (only dead cells stain blue).

RNA isolation and qRT-PCR

Total RNA was isolated using TRIzol (Invitrogen, Life Technologies, Carlsbad, CA, USA) according to the manufacturer's protocol. 1 µg of isolated RNA from each sample was used for cDNA synthesis using AMV reverse transcriptase (Roche Diagnostics GmbH, Mannheim, Germany), following the manufacturer's instructions. The reaction mixture was incubated 10 minutes at 25°C, 1 hour at 37°C, and 10 minutes at 72°C. The candidate genes were amplified in CFX96 Touch Real-Time PCR detection System (Bio-Rad) using 2 µl of cDNA, 400 nM forward and reverse primers (Supplementary Table S1), and 10 µl of SsoFast EvaGreen Supermix (Bio-Rad) in a final volume of 20 µl. Amplification was conducted according to the following conditions: 1) denaturation at 95°C for 10 min; 2) amplification for 60 cycles at 95°C for 10s, annealing temperature for 10s, 72°C for 10s; and 3) final extension at 72°C for 10 min. To quantify mRNA levels of the tested genes, the ΔCT method using a reference gene (GAPDH) was used, which is a variation of the Livak method. The results are presented as gene of interest/GAPDH, based on the formula $2^{-[C_T(target)-C_T(reference)]}$ [44].

Western blot analysis

Whole cell protein extract was obtained using RIPA buffer supplemented with protease inhibitor (Roche Diagnostics GmbH, Mannheim, Germany). The amount of 25 µg of each extracted protein sample was loaded onto fast cast SDS-PAGE gels based on the manufacturer's protocol (Bio-Rad). Next, the gel was positioned onto a TransBlot Turbo Polyvinylidene Fluoride (PVDF) membrane for protein transfer. This was done using Trans-Blot Turbo Transfer System (Bio-Rad). The Bio-Rad ChemiDoc imaging system was utilized to confirm successful protein transfer. Prior to overnight incubation at 4°C with the primary monoclonal antibody, anti-SIRT1 (diluted 1:10000, MilliporeSigma, #07–131), the membrane was blocked with EveryBlot Blocking Buffer for 5 minutes at room temperature. Next day, the membrane underwent 5–6 washes with TBS-Tween (TBST) buffer, following one hour of incubation at room temperature with the secondary antibody, horseradish peroxidase-conjugated

anti-rabbit IgG (diluted 1:1500; Cell Signaling, #7077). Using the Bio-Rad ChemiDoc imaging system, the total protein content was quantified to serve as a loading control for protein normalization, as previously described [45]. Chemiluminescent signals were captured on the ChemiDoc MP (Bio-Rad) after soaking the membrane with a 1:1 mixture of Clarity Western ECL Substrate (Bio-Rad) for 10 minutes. Band intensities were analyzed using Image Lab software (Bio-Rad).

DNA extraction and pyrosequencing

Genomic DNA from MCF10A cells was isolated after 20 hours of incubation of a cell lysate with proteinase K at 55°C, followed by extraction using a standard phenol:chloroform mixture (250 µl:250 µl), according to the manufacturer's protocol. Precipitated DNA was resuspended in TE buffer and stored at – 20°C. DNA bisulfite conversion was performed as previously described [38]. The process of DNA bisulfite conversion commenced with the incubation of DNA with a restriction enzyme EcoRI, followed by purification using the GeneJet PCR Purification Kit (Thermo Fisher Scientific). Upon treatment with sodium bisulfite, unmethylated cytosines are converted into uracil whereas methylated cytosines are preserved unaltered. Bisulfite converted DNA was further amplified using HotStar Taq DNA polymerase (Qiagen) and biotinylated primers for tested gene regulatory regions (Supplementary Table S1). The biotinylated DNA strands were pyrosequenced using the PyroMark Q48 AutoPrep instrument (Qiagen), according to the manufacturer's manual. The quantification of methylation percentage at a single CpG site resolution was conducted using PyroMark Q48 software.

Chromatin immunoprecipitation (ChIP) and quantitative ChIP (qChIP)

Chromatin immunoprecipitation (ChIP) assay was performed to determine DNA-protein interactions, as previously described [45]. Both control and PTS- or GEN-exposed human mammary epithelial MCF10A cells were fixed with 1% formaldehyde for 15 minutes at 37°C, incubated with PBS containing protease inhibitors, lysed and subjected to sonication. Samples were precleared with protein G agarose followed by centrifugation. The supernatants were divided into three sub-samples. The first sub-sample served as the input, while the second (negative control) and third sub-sample (experimental sample) were separately incubated overnight at 4°C with rabbit IgG non-specific antibody and anti-SIRT1 or anti-DNMT3B antibodies, respectively. Next, all sub-samples were washed, eluted, and utilized as a template for qPCR (qChIP), where the starting material in all conditions consisted of 25 ng of input, antibody-bound and IgG-bound DNA. The occupancy level of the proteins was expressed as (Bound-IgG)/Input. We used the following antibodies: anti-SIRT1 rabbit polyclonal (Millipore, #07–131), anti-DNMT3B rabbit mAb (Cell Signaling, #72335) and normal rabbit IgG (Cell Signaling, #2729). Primers used in qChIP are listed in Supplementary Table S1.

ChIP-re-ChIP assay (double-ChIP)

ChIP-re-ChIP assay was conducted following the procedure outlined previously [46]. In summary, MCF10A cells treated with 22 µM GEN for 9 days were fixed using 1% formaldehyde and divided into two equal samples. Sample #1 underwent immunoprecipitation with the anti-SIRT1 antibody followed by ChIP with the anti-DNMT3B antibody on SIRT1-bound fraction. Sample #2 was initially immunoprecipitated with the anti-DNMT3B antibody and next the DNMT3B-bound fraction was immunoprecipitated with the anti-SIRT1 antibody. Experimental steps followed the same workflow as in the single ChIP protocol described above in point 2.6 with a minor modification. After immunoprecipitation with the first antibody, 70% of the bound DNA fraction was dissociated from agarose beads, eluted and subjected to the incubation with the second antibody.

Small-interfering RNA (siRNA) transfection

Cells were plated at a density of 4 × 10^5 per a 10-cm tissue culture dish, 24 h prior to siRNA treatment. Control siRNA (si-CTRL, custom, antisense strand: 5'-UCGCCUAGGCUGCCAAGGCUU-3') and human SIRT1 siRNA (si-SIRT1, SMARTpool

M-003540-01-0005) were purchased from Dharmacon. Cells were transfected with siRNA using Lipofectamine RNAiMAX (Invitrogen, Carlsbad, CA) prepared in serum-free Opti-MEM. In brief, 15 µl of Lipofectamine was incubated in 500 µl of Opti-MEM for 45 minutes at room temperature. A concentration of 56 nM siRNAs was added to the Lipofectamine-Opti-MEM solution followed by a 15-minute incubation at room temperature. This mixture was then added to cells in 4 ml of Opti-MEM. The transfection solution was removed after 5 hours of incubation at 37°C and replaced with a fresh medium. GEN was added next morning at 22 µM concentration. After 2 days, cells were split 1:2 and 24 h later the second transfection and treatment with GEN were performed following the same protocol. Cell were harvested and subjected to RNA and protein isolation for further analyses.

Analysis of publicly available gene expression databases

To evaluate whether the selected genes, *rDNA*, *RNF114*, and *RNF169*, are clinically relevant, we screened publicly available data using GEO2R (http://www.ncbi.nlm.nih.gov/geo/geo2r/), an interactive web tool for comparing two groups of data to analyze any GEO series [47], and GENT2 (http://gent2.appex.kr/gent2/), a gene expression database for normal and tumor tissues [48]. Expression data from publicly available datasets are presented in boxplots and depict minimum, interquartile range (IQR), and maximum. Statistical analyses on the data were performed using Mann-Whitney *U* test for sets with two groups and two-sample T-test for the overall analysis of expression data across different tissues (GENT2).

Statistical analysis

In statistical analyses, the unpaired t-test with a two-tailed distribution was applied for comparisons between two groups. One-way analysis of variance (ANOVA) with Tukey post-hoc test was used to analyze and compare multiple groups in western blotting, qRT-PCR, pyrosequencing, ChIP-re-ChIP, and siRNA transfection. All values are presented as the mean ± S.D. of three independent experiments. Results were considered statistically significant when $p < 0.05$.

Results

Putative phytoestrogen-target genes selected from existing datasets

Upon the integration of data from two genome-wide datasets, as described in Materials and Methods, we identified a set of genes that are differentially methylated and/or expressed in response to phytoestrogens in normal experimental models. We refer to these genes as 'phytoestrogen-target genes.' A detailed functional analysis show that phytoestrogen-target genes are enriched with biological processes and functions that are related to cellular homeostasis and health maintenance, including regulation of the inflammatory response, cell survival and healing, DNA repair, protein homeostasis (i.e., proteostasis), cell proliferation and motility, genomic integrity, and regulation of immune functions (Table 1).

Increased mitochondrial biogenesis was one of the identified functions, and included *DAO* as a hypermethylated and thus potentially down-regulated phytoestrogen-target gene. *DAO* is a D-amino acid oxidase, deaminating D-amino acids with a concomitant reduction of FAD to FADH2. Subsequent re-oxidation of FADH2 by molecular oxygen produces H2O2, which induces oxidative stress and reactive oxygen species (ROS) production [49,50]. High ROS levels affect mitochondrial respiration and fusion leaving mitochondria fragmented and aggregated.

In the category of cell survival and wound healing, we found *FGFR1OP2* and *MMP13*, which were hypomethylated in our dataset, and could potentially lead to their upregulation in response to phytoestrogens (Table 1). FGFR1OP2, that belongs to a fibroblast growth factor (FGF) family, has been shown to facilitate fibroblast-driven wound closure and accelerate the process of healing [51]. Similarly, MMP13 is a member of the matrix metalloproteinases (MMPs) family that plays an essential role in wound re-epithelialization [52], promotes survival of human skin fibroblasts and regulates wound granulation [53].

Numerous phytoestrogen-target genes were enriched with functions linked to regulation of the inflammatory response. We found glutathione S-transferases, theta 1 (*GSTT1*) and pi 1 (*Gstp1*), to be hypermethylated and downregulated, respectively, in response to phytoestrogens in normal models (Table 1). GSTP1 has been shown to inhibit inflammation by buffering and reducing ROS, it is highly expressed in certain types of cancer [54]. The same observation was noted for GSTT1 that was recently reported to be a mediator of metastasis [55], although previous studies have demonstrated that lack of GSTT1 May be linked to increased susceptibility to inflammatory disease [56]. Suppressive effects of these enzymes on the inflammatory pathways may be advantageous during cell transformation. Hence, their downregulation by phytoestrogens could contribute to maintaining homeostasis in the cellular response to inflammation and transformation.

We found many genes linked to immune functions among phytoestrogen-target genes (Table 1). For instance, hypomethylated and thereby potentially upregulated *BCL6* regulates the transcriptional program of innate lymphoid cells that are effector cells essential for tissue homeostasis, protective immunity, and inflammatory regulation [57]. Potential upregulation of *BCL6* by phytoestrogens could be vital to cellular homeostasis. Another phytoestrogen-target gene linked to transcriptional regulation is *EBF4*, a transcription factor whose knockout inhibits apoptosis of immune cells [58]. Hence, *EBF4* hypermethylation in response to phytoestrogens, potentially leading to reduced expression, could indicate protective effects towards immune cells.

Interestingly, a gene family represented by several members in the two analyzed datasets was E3 ubiquitin protein ligase RNF. *RNF169* was hypermethylated and thus potentially downregulated in response to RSV in MCF10A cells, whereas *Rnf5* and *Rnf114* were downregulated upon PTS supplementation in rat blood. All RNF members are involved in protein homeostasis via regulating ubiquitination-dependent protein stability/function and ubiquitination-dependent protein catabolic process. As E3 ubiquitin ligases target a variety of substrates, they are involved in numerous cellular processes including DNA repair, programmed cell death, and metabolism [59,60]. RNF169 negatively regulates double-stranded DNA break repair processes as it competitively interferes with the recruitment of DNA repair factors [59]. On the other hand, RNF114 has been shown to facilitate double-stranded DNA break repair by recruiting central components of the repair machinery [60]. Both RNF169 and RNF114 could contribute to the maintenance of genomic stability through regulating the DNA damage response. In addition, RNF114 regulates the immune and inflammatory responses via attenuating NFκB-dependent functions in T cells [61] but enhancing NFκB and the innate immune response in epithelial inflammation [62]. Similarly, RNF5 is involved in the regulation of the immune response; it decreases the immune functions via interfering with autophagosome formation, which diminishes autophagy [63].

While investigating the top differentially expressed gene, *rDNA*, was found to be downregulated by 30-fold in response to PTS in rat blood. It encodes for ribosomal RNA (rRNA), namely 45S rRNA precursor that is transcribed as one transcription unit and processed later to 18S, 5.8S and 28S rRNAs [64]. Ribosomal RNAs are integral part of the ribosome which is the translation machinery for protein synthesis [64]. Although ribosome biogenesis is essential for cell growth and tissue formation throughout fetal growth and development, it inversely correlates with longevity in post-developmental phase and was shown to be enhanced in premature aging [65,66].

Considering the magnitude of differential DNA methylation or gene expression, functions, and enrichment of the entire gene family in the analyzed genome-wide datasets, we have selected *RNF114*, *RNF169* and *rDNA* as candidate genes for further mechanistic investigations into phytoestrogens' health effects. While *rDNA* is the top differentially expressed gene, *RNF169* takes the seventh position out of 100 differentially methylated genes. Both *RNF114* and *RNF169* belong to the same gene family but were not identified in the same dataset. All three putative targets of phytoestrogens are linked to several biological functions implicated in health maintenance, including genome stability, DNA repair, and protein homeostasis (Table 1).

Although phytoestrogens may have distinct functions in normal versus diseased cells (e.g.,

cancer cells), phytoestrogen-mediated downregulation of the selected targets appears to be clinically significant as well. First, enhanced ribosomal biogenesis and rRNA production are crucial for supporting increased cellular activities of cancer cells [67]. Second, upregulation of *RNF* genes enables cancer cells to maintain protein stability and sustain catabolic processes in the environment of increased protein synthesis and turnover [68]. Indeed, upon screening publicly available datasets, we found that *rDNA* and *RNF114* are upregulated in breast tumors as compared to normal mammary epithelium (Supplementary Figure S1A,B). While *rDNA* expression data across tissues was not available in GENT2 database, expression of *RNF114* showed an overall increase in tumors versus normal tissues (Supplementary Figure S1C). Although we have not identified any available GEO dataset where *RNF169* would be upregulated in breast cancer, *RNF169* expression across different cancer types was upregulated as compared with normal tissues (Supplementary Figure S1D). Furthermore, we detected increased *RNF169* expression in skeletal muscle of older non-trained individuals (lack of exercise) compared to young trained individuals (Supplementary Figure S1E), which implies that RNF169 is linked to disturbed homeostasis and impaired health status.

Dose-dependent effects of pterostilbene (PTS) or genistein (GEN) on growth of human MCF10A mammary epithelial cells

Using a prolonged 9-day treatment schedule to more closely reflect habitual exposures to low doses of dietary bioactive compounds in humans, we established non-toxic doses of PTS and GEN that exhibit effect on MCF10A mammary epithelial cell growth. We initially subjected MCF10A cells to PTS or GEN at increasing concentrations, ranging from 0 to 20 μM or 0 to 40 μM, respectively (Figure 1(a,b)). With increasing concentrations, we observed a dose-dependent inhibitory effects on MCF10A cell growth after 4-day and 9-day exposure (Figure 1(a,b)). Based on the dose-response, we determined that PTS at 7 μM and GEN at 8 μM decrease cell number by approximately 25% compared to vehicle-treated control cells on day 9 (IC25). PTS at 11 μM and GEN at 22 μM were established as IC50 values, which produce 50% inhibition of cell growth. Treatments at the established IC25 and IC50 concentrations showed that cell growth was significantly inhibited by approximately 22% at 7 μM PTS and 52% at 11 μM PTS, as compared with control cells (Figure 1(a), right panel). GEN at 8 μM and 22 μM led on average to 20% and 50% inhibition, respectively (Figure 1(b), right panel). The IC25 and IC50 doses were non-toxic and resulted in less than 10% of dead cells.

SIRT1 protein level, but not mRNA level, is increased by pterostilbene (PTS) or genistein (GEN) in human MCF10A mammary epithelial cells

To test our hypothesis on the role of SIRT1 in phytoestrogens' effects, we subsequently investigated the impact of PTS and GEN on *SIRT1* expression at both mRNA and protein levels in MCF10A cells. Following a 9-day exposure to PTS or GEN, no significant changes in *SIRT1* mRNA level were observed at any of the applied concentrations, as compared to the control cells (Figure 1(c,d)). However, both compounds at higher IC50 concentrations led to an increase in SIRT1 protein. Treatment with PTS at 11 μM resulted in a 59% increase in SIRT1 protein level (Figure 1(e)), while 22 μM GEN led to approximately a 68% SIRT1 increase, as compared to vehicle-treated control cells (Figure 1(f)).

SIRT1 occupancy is consistently increased at all target genes in response to genistein (GEN), but not pterostilbene (PTS), in human MCF10A mammary epithelial cells

PTS and GEN at IC50 concentrations led to an increase in SIRT1 protein level. However, changes in SIRT1 levels may not reflect a functional role of SIRT1 which is associated, at least partially, with SIRT1 binding to DNA. Thus, we used ChIP to measure SIRT1 occupancy at promoters of the selected phytoestrogen-target genes, namely *RNF114*, *RNF169* and *rDNA*, in MCF10A cells upon 9-day exposure to IC25 and IC50 doses of PTS and GEN (Figure 2). Within the *RNF114* promoter region, SIRT1 occupancy did not increase

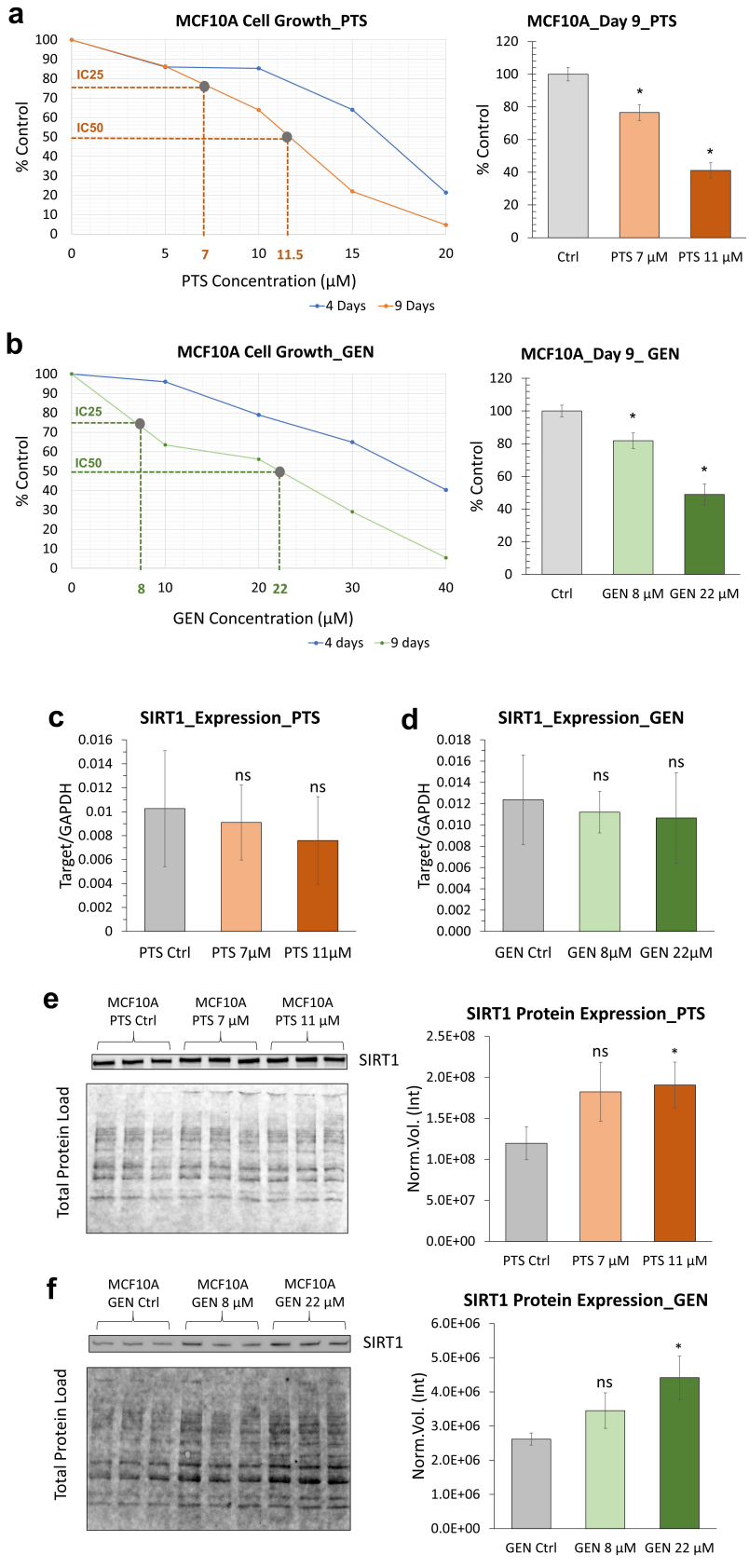

Figure 1. Impact of pterostilbene (PTS) or genistein (GEN) on cell growth and SIRT1 expression in MCF10A mammary epithelial cells. (a,b) MCF10A cell growth in response to different PTS (a) or GEN (b) concentrations upon 4- and 9-day exposure. Bar charts show MCF10A cell growth in response to 9-day exposure to 7 μM and 11 μM PTS (a) or 8 μM and 22 μM GEN (b), as compared with vehicle-treated cells (ctrl, ethanol for PTS and DMSO for GEN). All results were determined by the trypan blue exclusion test, and cell number

after exposure to 7 μM PTS (Figure 2(a) upper panel). However, there was an obvious enrichment at 11 μM PTS, demonstrating an approximately 5.7-fold increase in SIRT1 binding compared to the control cells (Figure 2(a), lower panel). Interestingly, while SIRT1 binding was not detectable in control cells, PTS at both 7 μM and 11 μM concentrations resulted in a robust increase of SIRT1 occupancy at the *RNF169* promoter region (Figure 2(b)). Conversely, no significant changes in SIRT1 binding were observed within the *rDNA* promoter in response to PTS (Figure 2(c)).

Contrary to PTS, 9-day treatment with GEN resulted in SIRT1 increase at promoters of all tested genes, regardless of its concentration (Figure 2(d-f)). SIRT1 binding increased by 2.2-fold in *RNF114* promoter upon treatment with 8 μM GEN (Figure 2(d), upper panel). While there was very low binding at *RNF169* and *rDNA* in control cells, we detected clear SIRT1 enrichment at these two genes in response to 8 μM GEN (Figure 2(e,f), upper panels). There was approximately a 2.7-, 5.6-, and 3.5-fold increase in SIRT1 occupancy at *RNF114*, *RNF169*, and *rDNA* promoters, respectively, upon exposure to 22 μM GEN (Figure 2 (d–f), lower panels).

Expression of RNF169 *and rDNA, but not RNF114, is downregulated in response to pterostilbene (PTS) and genistein (GEN) in human MCF10A mammary epithelial cells*

SIRT1 acts as a histone deacetylase which consequently may result in a condensed chromatin structure. To explore whether SIRT1 binding to gene promoters in response to PTS or GEN is accompanied by downregulation of gene expression, we assessed the mRNA levels of the target genes using qRT-PCR. While *RNF114* expression exhibited no significant variations in response to either PTS or GEN (Figure 3(a,b)), a distinct pattern emerged for *RNF169* and *rDNA*. *RNF169* expression was significantly reduced by 40% and 21% in response to 11 μM PTS and 22 μM GEN, respectively (Figure 3(a,b)). Similarly, there was a marked downregulation by 25% and 32% for *rDNA* in response to 11 μM PTS and 22 μM GEN, respectively (Figure 3(a,b)). The lower 7 μM dose of PTS selectively led to *RNF169* downregulation only, without influencing the expression level of *rDNA* (Figure 3(a)). GEN at the lower 8 μM dose did not lead to changes in *RNF169* or *rDNA* expression (Figure 3(b)).

Taking into consideration changes in expression levels, only *RNF169* and *rDNA* were further investigated to elucidate the role of SIRT1 in PTS- and GEN-mediated epigenetic regulation of gene expression.

Differential DNA methylation within promoters of the target genes in response to pterostilbene (PTS) or genistein (GEN) in human MCF10A mammary epithelial cells

Since SIRT1 was shown to interact with DNMT3B DNA methyltransferase at gene-specific loci [8], we next determined whether SIRT1 binding at promoters of the selected genes and decreased gene expression are associated with the increased promoter DNA methylation in response to PTS or GEN. To do this, we used pyrosequencing technology to quantitatively assess the percentage of DNA methylation at a single CpG site resolution. Three CpG sites and seven CpG sites were assessed within the *RNF169* and *rDNA* promoter regions, respectively. CpG sites were selected based on our genome-wide DNA methylation dataset (*RNF169*) or literature (*rDNA*) (Figure 3(c)). Exposure of MCF10A cells to 22 μM GEN resulted in a significant 22% increase in methylation at CpG #2 of *RNF169* on day 9 (Figure 3(e), left panel), whereas no such effect was observed for PTS

is expressed as a percentage of control. (c,e) *SIRT1* gene expression at mRNA (c) and protein levels (e) in MCF10A cells upon 9-day exposure to PTS at 7 μM and 11 μM. (d,f) *SIRT1* mRNA expression (d) and protein levels (f) in MCF10A cells upon 9-day exposure to GEN at 8 μM and 22 μM. Results were determined by qRT-pcr and western blot. In western blot analyses, reactive bands were visualized using the chemiluminescent protocol in the ChemiDoc MP imaging system (bio-rad) and analyzed using the image lab software. Protein loading was normalized with respect to total sample protein loaded using free stain gels. All results represent mean ± SD of three independent experiments. $^{*}p < 0.05$.

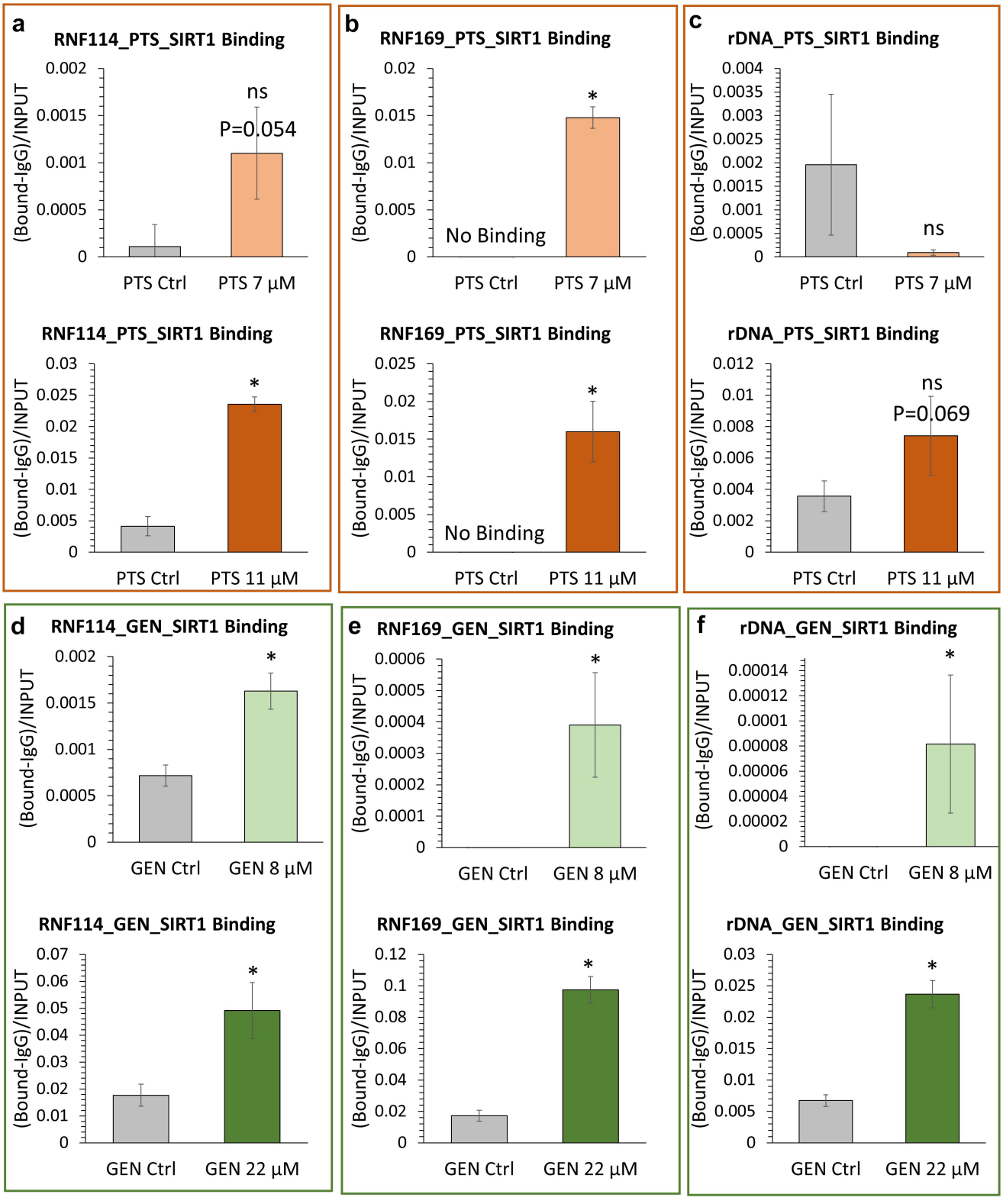

Figure 2. SIRT1 binding at RNF114, RNF169 and rDNA promoters upon 9-day exposure to PTS or GEN in MCF10A cells. (a-c) SIRT1 binding after 9-day exposure to 7 µM and 11 µM PTS at *RNF114* (a), *RNF169* (b), and *rDNA* (c) promoters. (d-f) SIRT1 binding after 9-day exposure to 8 µM and 22 µM GEN at *RNF114* (d), *RNF169* (e), and *rDNA* (f) promoters. All results were determined by quantitative chromatin immunoprecipitation (qChIP), and represent mean ± SD of three independent experiments. *$p < 0.05$.

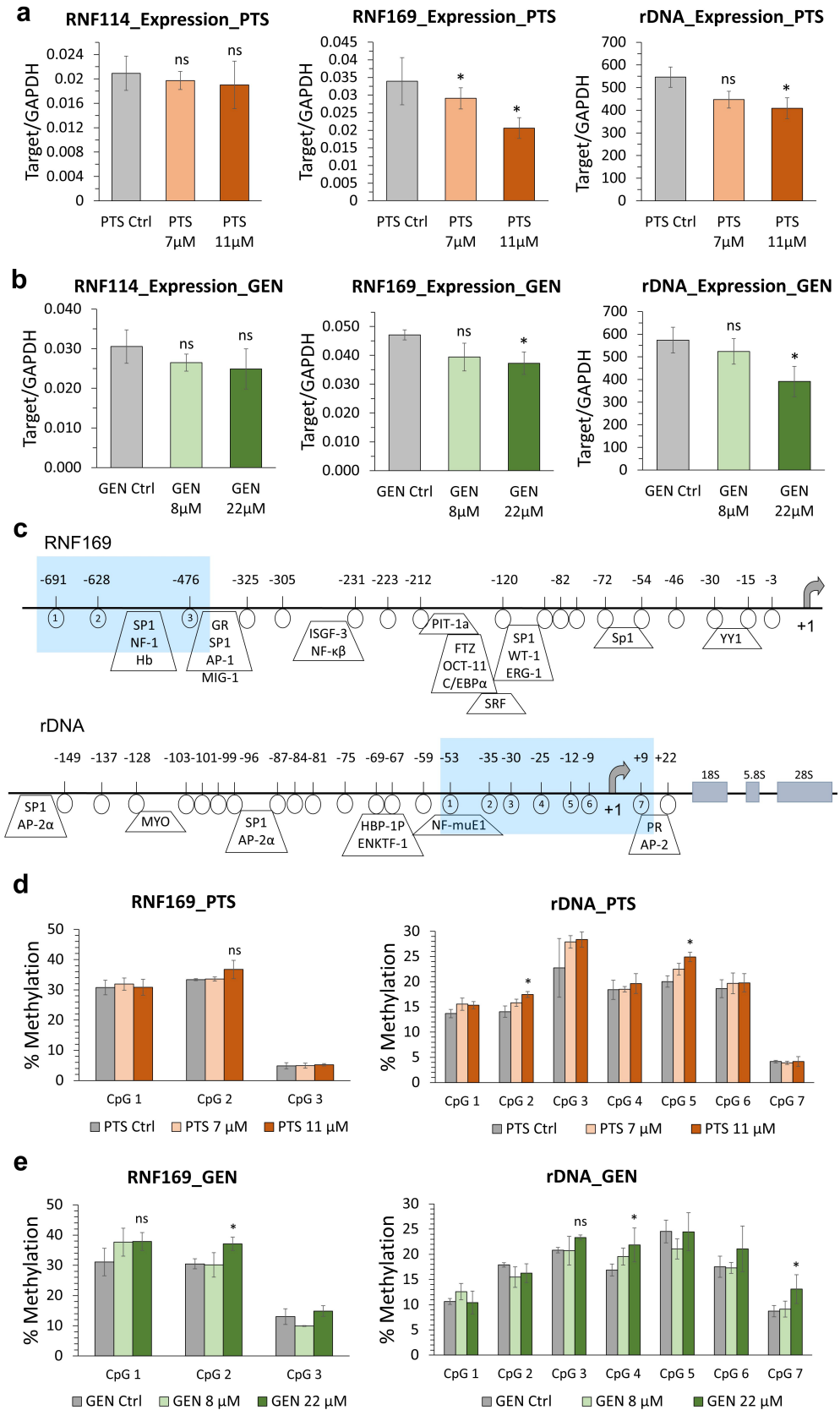

Figure 3. PTS- and gen-mediated changes in gene expression and DNA methylation of target genes in MCF10A cells. (a-b) expression at mRNA levels for *RNF114*, *RNF169* and *rDNA* upon 9-day exposure to 7 μM and 11 μM PTS (a), and 8 μM and 22 μM GEN (b) in MCF10A cells as determined by qRT-pcr. (c Maps of promoter regions of *RNF169* and *rDNA*, where the light blue shaded area represents the CpG sites tested by pyrosequencing (numbered CpGs). (d-e) average methylation status of CpG sites within *RNF169* and *rDNA* promoters in MCF10A cells after 9-day exposure to 7 μM and 11 μM PTS (d) or 8 μM and 22 μM GEN (e), as determined by pyrosequencing. All results represent mean ± SD of three independent experiments. *$p < 0.05$.

(Figure 3(d), left panel). With respect to *rDNA*, both PTS and GEN resulted in hypermethylation across different CpG sites (Figure 3(d,e), right panel). After exposing MCF10A cells to 11 μM PTS for 9 days, we noted a ~ 24% increase in DNA methylation at CpG #2 and CpG #5 within *rDNA* promoter (Figure 3(d), right panel). Upon 22 μM GEN, in turn, significant increases in DNA methylation of *rDNA* promoter were observed at CpG #4 (by 30%) and CpG #7 (by 50%) (Figure 3 (e), right panel). These hypermethylation events were detected only upon exposure to higher doses of the compounds, IC50 concentrations, and correlated with gene downregulation.

DNMT3B occupancy increases at RNF169 and rDNA promoters in response to genistein (GEN), but not pterostilbene (PTS), in human MCF10A mammary epithelial cells

Since we observed DNA hypermethylation at several SIRT1-occupied gene regions following 9-day exposure of MCF10A cells to PTS or GEN, we proceeded with the evaluation of DNMT3B binding at the regulatory regions of the tested genes using qChIP. DNMT3B was selected among DNA methyltransferases as it was previously shown that SIRT1 facilitates DNMT3B recruitment to DNA and subsequent DNA methylation [7]. In addition, we previously reported on DNMT3B as a required enzyme for PTS-mediated hypermethylation of oncogenes in breast cancer cells [39]. Interestingly, the increased DNMT3B occupancy was consistently observed in response to GEN, but not PTS (Figure 4(a–d)). Strikingly, no binding of DNMT3B was detected for *rDNA* upon exposure to PTS (Figure 4(b)). Within the *RNF169* promoter, 38% and 90% reduction, rather than an increase, in DNMT3B binding was detected in response to 7 μM and 11 μM PTS, respectively (Figure 4(a)). On the contrary, GEN at both 8 μM and 22 μM concentrations resulted in a robust enrichment in DNMT3B binding at *rDNA*, as compared with control cells where no binding was detected (Figure 4 (d)). Within the *RNF169* promoter region, a substantial 27-fold increase in DNMT3B occupancy was observed upon exposure to 22 μM GEN, whereas a lower dose produced a statistically non-significant increase (Figure 4(c)).

SIRT1 and DNMT3B do not co-occupy RNF169 *and rDNA promoter regions in response to genistein (GEN) in human MCF10A mammary epithelial cells*

Prior studies suggest that SIRT1 serves as a platform for recruiting DNA methylating enzymes like DNMT3B, ultimately facilitating DNA methylation [7]. Our results have demonstrated an enrichment of both SIRT1 and DNMT3B binding at *RNF169* and *rDNA* promoters when MCF10A cells are exposed to 22 μM GEN for 9 days. Intrigued by these findings, we sought to investigate whether DNMT3B and SIRT1 co-bind the same DNA loci in response to GEN to remodel gene transcription. To explore it, we used a ChIP-re-ChIP (or double ChIP) assay paired with quantitative PCR analysis of the input and bound samples upon single ChIP with protein 1 (SIRT1 or DNMT3B) and re-ChIP with protein 2 (DNMT3B or SIRT1, respectively) on the protein 1-bound fraction [46]. In ChIP-re-ChIP, if levels of enrichment are higher than those of single ChIPs, full co-occupancy is concluded. As shown in Figure 4(e), in single ChIP analysis, SIRT1 (grey bars) and DNMT3B (white bars) bind to promoters of *RNF169* and *rDNA*. However, in the ChIP-re-ChIP analysis, SIRT1 and DNMT3B are not co-enriched at either of the gene promoters; profoundly lower levels of enrichment than those of single ChIPs are observed regardless of the order of performance of the two immunoprecipitations (black and pattern bars in Figure 4(e)).

SIRT1 is required for genistein (GEN)-mediated downregulation of rDNA, but not RNF169*, in human MCF10A mammary epithelial cells*

To assess whether SIRT1 is required for GEN-mediated epigenetic regulation of gene transcription, we performed transfection of MCF10A cells with *SIRT1*-siRNA to deplete *SIRT1*. Using qRT-PCR and western blot, we confirmed a significant 75% reduction of mRNA level and 99% decrease in protein level of *SIRT1* upon *SIRT1*-targeting siRNA treatment, as compared with cells treated

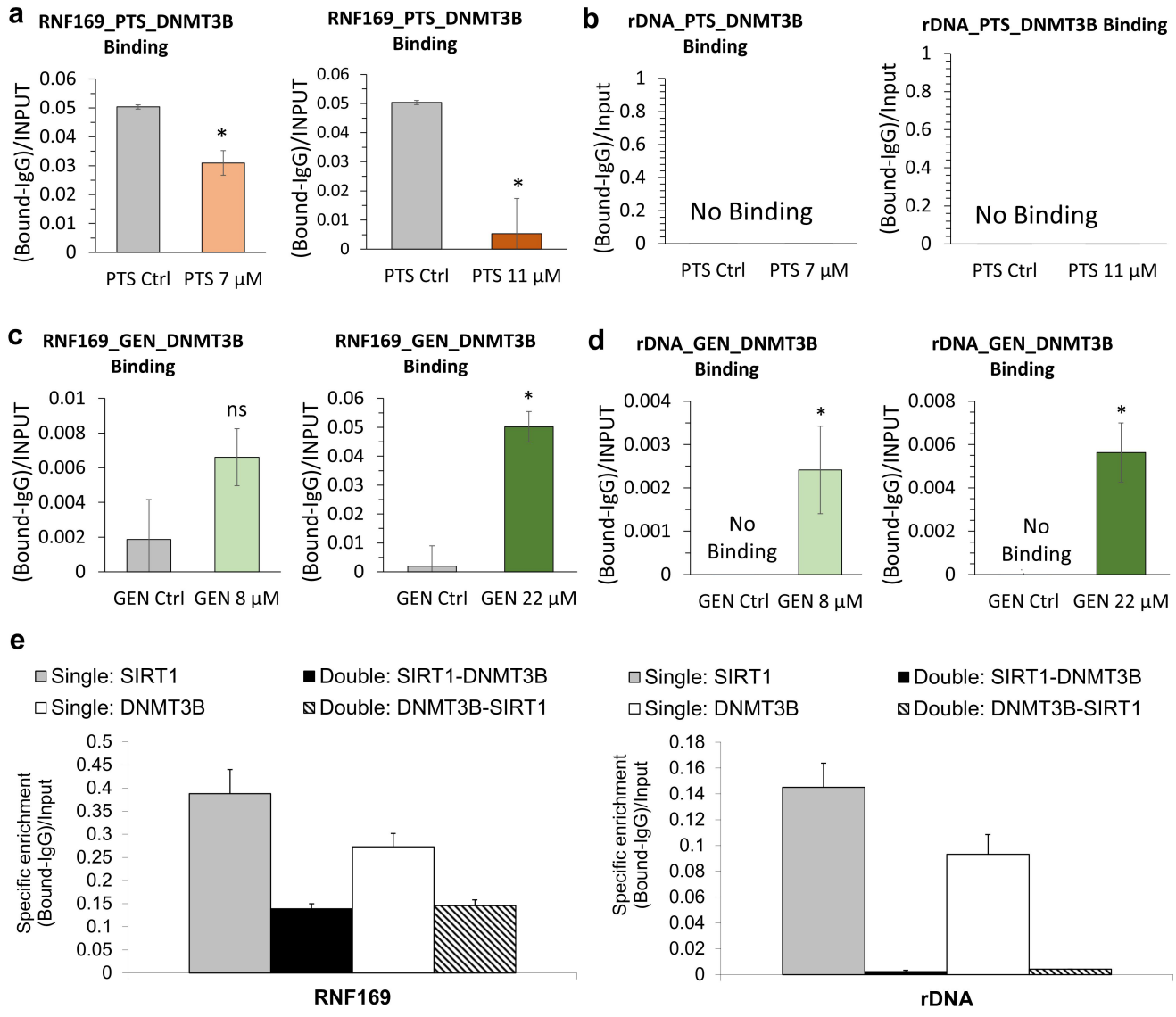

Figure 4. DNMT3B binding and SIRT1-DNMT3B co-occupancy at *RNF169* and *rDNA* promoters upon 9-day exposure to PTS or GEN in MCF10A cells. (a,b) DNMT3B binding after 9-day exposure to 7 μM and 11 μM PTS at *RNF169* (a) and *rDNA* (b) promoters. (c,d) DNMT3B binding after 9-day exposure to 8 μM and 22 μM GEN at *RNF169* (c) and *rDNA* (d) promoters. All results were determined by quantitative chromatin immunoprecipitation (qChIP). (e) ChIP-re-ChIP assay was used to determine co-occupancy of SIRT1 and DNMT3B at *RNF169* and *rDNA* promoters in response to 9-day exposure to 22 μM GEN. 'Double: SIRT1-DNMT3B' refers to SIRT1 binding first followed by DNMT3B binding; 'double: DNMT3B-SIRT1' indicates the reverse order. The sequential binding orders at the same region can be identified. Results were quantified by quantitative PCR. All results represent mean ± SD of three independent experiments. *$p < 0.05$.

with control siRNA, si-Ctrl (Figure 5(a,b)). The level of *SIRT1* expression remained low and unchanged even after GEN treatment (Figure 5 (a)). Interestingly, we found that *SIRT1* depletion abrogated GEN-mediated downregulation of *rDNA* expression, providing a mechanistic proof for a requirement of SIRT1 in GEN-mediated *rDNA* transcriptional regulation (Figure 5(d)). On the other hand, despite *SIRT1* knockdown, GEN still led to downregulation of *RNF169*, suggesting that there is an alternative mechanism of transcriptional regulation of *RNF169* expression in response to GEN (Figure 5(c)).

Discussion

Our previous omics datasets indicate phytoestrogen-target genes are implicated in processes

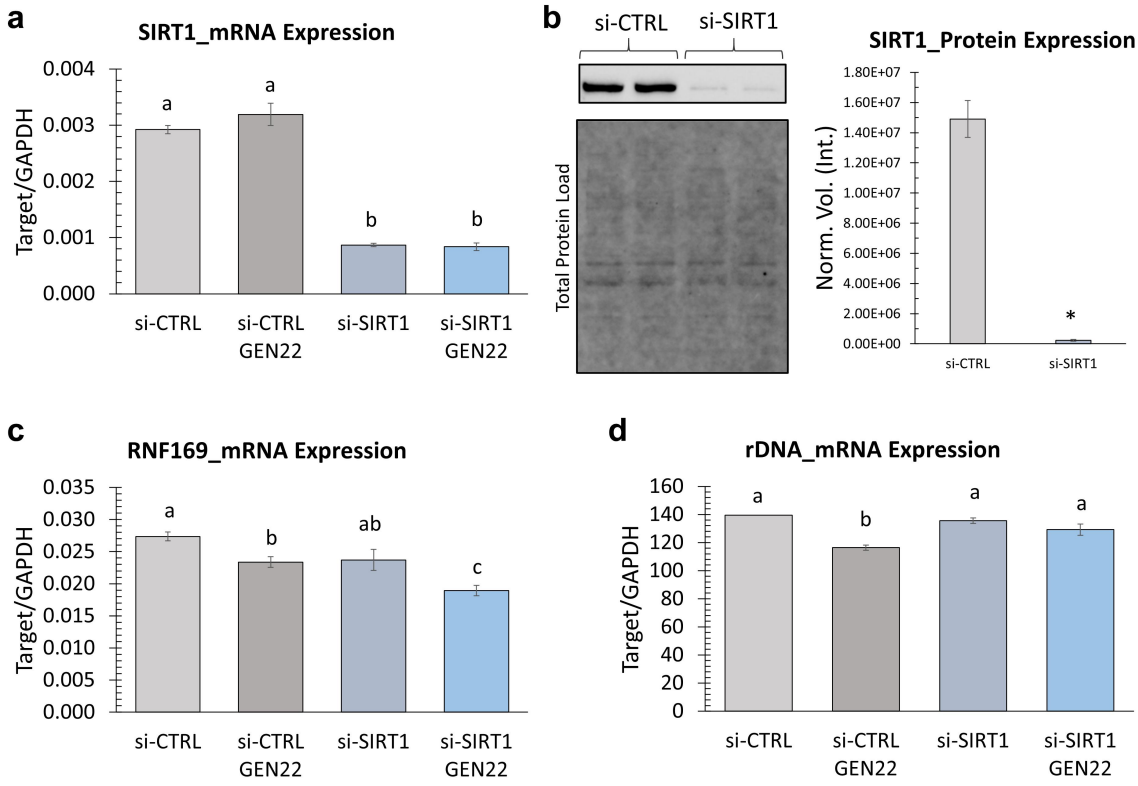

Figure 5. Expression of *SIRT1*, *RNF169* and *rDNA* upon 9-day exposure to 22 μM GEN in MCF10A cells upon *SIRT1* depletion. MCF10A cells were transfected with control siRNA and siRNA targeting *SIRT1* followed by exposure to 22 μM GEN. (a-b) expression of SIRT1 at mRNA (a) and protein (b) level, as determined by qRT-pcr and western blot, respectively. (c-d) expression of *RNF169* (c), and *rDNA* (d) at mRNA levels, as determined by qRT-pcr. All results represent mean ± SD of three independent experiments. *$p < 0.05$.

and functions that are linked to cellular homeostasis and health maintenance, such as regulation of the inflammatory response, oxidative stress, DNA repair, immune functions, and genome stability (Table 1). In the present study, we used a well-characterized human mammary epithelial cell model, MCF10A, to explore how phytoestrogens epigenetically impact cell biology to maintain cellular homeostasis. We found that exposure to PTS or GEN resulted in decreased expression of *RNF169* and *rDNA*, which was accompanied by increased SIRT1 occupancy at *RNF169* after PTS, and at both *RNF169* and *rDNA* after GEN. Increase in SIRT1 enrichment was associated with both DNMT3B binding and hypermethylation of the gene promoters only in response to GEN. Although PTS led to increased DNA methylation within *rDNA*, DNMT3B binding was not detected. Furthermore, we mechanistically established that GEN-mediated suppression of *rDNA* transcription requires SIRT1. Our findings demonstrate a distinct mechanism of action of GEN and PTS in epigenetic suppression of genes functionally linked to disrupted cellular homeostasis. As the present study was performed using one cell line, we recognize that further investigation is warranted to validate GEN and PTS action in other normal models.

We hypothesized that SIRT1 is involved in epigenetic effects mediated by PTS and GEN in mammary epithelial cells. Although the compounds did not change *SIRT1* mRNA levels (Figure 1(c,d)), they led to higher SIRT1 protein levels (Figure 1 (e,f)) and enriched SIRT1 occupancy at promoters of all (GEN) or some (PTS) target genes (Figure 2). Previous studies have shown that 17β-estradiol upregulates *SIRT1* via ERα, and can allosterically activate SIRT1 via binding to its N-terminal domain in breast cancer cells [69,70]. Considering the structural similarity between phytoestrogens and 17β-estradiol, it is plausible that phytoestrogens mimic effects of 17β-estradiol on SIRT1. Although MCF10A cells, our experimental

model, are ER-negative, they possess an active alternative estrogen signaling pathway mediated by GPER [71]. Of note, 17β-estradiol was demonstrated to also act through GPER to activate the EGFR/ERK/c-fos/AP-1 transduction pathway, inducing SIRT1 expression in ER-negative cancer cells [69].

Considering the estrogen receptor status, the content of phenol red in the culture media becomes an interesting aspect. In our study, MCF10A cells were cultured in DMEM/F12 (1:1) medium (Gibco) that contains 8 mg/L of phenol red. It was reported that phenol red acts as a weak estrogen and affects growth of ER-positive MCF7 breast cancer cells at 5 mg/L after 60 hrs of culture; however, this effect was only observed in the presence of high serum concentration (20%) [72]. In contrast, at the 5% serum concentration used in our experiments, a much higher concentration of 20 mg/L of phenol red was needed to observe an effect on cell growth. Moreover, phenol red was found to have no effect on ER-negative MDA-MB -231 cells [73]. As MCF10A cells are ER negative and grow at 5% of serum, the effect of phenol red at 8 mg/L in our experimental model should be minimal, if any. Nevertheless, as MCF10A cells have active GPER [71] and the activity of phenol red via GPER remains unknown, we cannot rule out the potential estrogenic effects of phenol red. Future studies should also consider whether phenol red impacts the action of phytoestrogens.

Apart from the action via estrogen receptors, the increase in SIRT1 protein level in response to phytoestrogens in our study may also be attributed to other regulatory mechanisms, including post-translational modifications like ubiquitination and post-transcriptional events such as regulation of mRNA stability [74]. Indeed, a decrease in SIRT1 protein ubiquitination may reduce subsequent SIRT1 degradation and thus increase SIRT1 protein levels [75]. Furthermore, increased mRNA stability was shown to enhance SIRT1 translation and thus protein levels [76]. Interestingly, a developing field of epitranscriptomics addresses regulation of RNA stability through post-transcriptional epigenetic modifications on RNA molecules [77]. A recent study demonstrates a crucial role of epitranscriptomic modifications in mediating dietary effects on health [78]. Specifically, in mice fed a high-fat diet, disrupted gut microbiome resulted in decreased methylation of adenine on mRNA (m6A) within regulators of the anti-obesogenic gut hormone GLP1, leading to suppression of the hormone [78]. Although the evidence for the impact of phytoestrogens on epitranscriptomics remains limited, GEN was demonstrated to increase expression of m6A RNA demethylase, ALKBH5, in a mouse model of renal fibrosis, leading to reduced total m6A levels and suppression of factors controlling epithelial-mesenchymal transition [79].

In our current study, downregulation of *rDNA* was accompanied by increased DNA methylation levels at *rDNA* promoter region in response to PTS and GEN (Figure 3(d,e)). A similar correlation was observed for *RNF169* but only in response to GEN (Figure 3(e)). Indeed, it is well-established that DNA methylation at gene regulatory regions is associated with transcriptional silencing [3]. Of note, although we detected decreased mRNA levels of *RNF169* in response to PTS at both IC25 and IC50 concentrations (Figure 3(a)), there were no significant changes in *RNF169* promoter methylation (Figure 3(d)). This discrepancy may arise from the involvement of an alternative epigenetic mechanism, including histone modifications. SIRT1 binding to *RNF169* in response to PTS (Figure 2(b)) may be sufficient to deacetylate histones and form condensed chromatin. A recent study shows that deacetylation of histone H4 inhibits the elongation of RNA polymerase II, thereby reducing the transcription activity of a target gene [9]. Additionally, other repressive histone marks such as tri-methylation of lysine 27 at histone H3 (H3K27me3) may be deposited at the *RNF169* locus, leading to a more condensed chromatin state [6].

Interestingly, although SIRT1 binding was detected at the *RNF114* promoter in response to both compounds, neither PTS nor GEN reduced expression of the gene. For this reason, we excluded *RNF114* from further analyses. We concluded that changes in DNA methylation, if any, would not be biologically meaningful. Nevertheless, in future studies, it would still be interesting to explore DNA methylation and DNMT3B binding within *RNF114* promoter and

investigate whether a chromatin-remodeling complex (e.g., B-WICH shifting from NuRD) [80] or transcriptionally active chromatin loops [81] are potentially involved in shielding the *RNF114* promoter from transcriptional suppression in response to phytoestrogens.

The interaction between SIRT1 and DNMT3B has been elucidated in several studies. Initially, SIRT1 was found to co-immunoprecipitate with DNMT3B, contributing to the maintenance of a repressed state of pro-inflammatory genes during macrophage differentiation [7,8]. SIRT1 also facilitated the recruitment of DNMT3B through histone deacetylation, leading to subsequent DNA methylation within the nucleus of embryonic stem cells [8]. Furthermore, DNMT3B and SIRT1 were shown to be transiently recruited to the induced DNA break loci at the promoter of *E-cadherin* gene. However, the recruitment of DNMT3B appears to rely on the presence of SIRT1, as DNMT3B is not enriched at the break sites when SIRT1 is knocked down [10]. While co-immunoprecipitation uses an antibody to purify its target antigen (protein of interest) along with its binding partners from a mixed sample, the ChIP-re-ChIP assay (double ChIP), we applied in our study, allows for the investigation of the sequential binding of SIRT1 and DNMTB to the same DNA locus. Hence, ChIP-re-ChIP provides insights into the combinatorial patterns of protein-DNA interactions, which constitutes a strength of our study. Interestingly, although both SIRT1 and DNMT3B bind *RNF169* and *rDNA* promoters in response to GEN, the ChIP-re-ChIP analysis shows that they do not co-occupy the same DNA locus (Figure 4(e)). We could speculate that SIRT1 binds first and subsequent histone deacetylation is recognized by DNMT3B facilitating its recruitment. Indeed, it was demonstrated that DNMT3B binding is enriched within hypoacetylated and condensed chromatin [8]. Results depicted in Figures 2(d–f) and 4(c) appear to support the scenario of SIRT1 binding first, as IC25 dose of GEN is sufficient for SIRT1 binding, however, a higher IC50 concentration is required to detect consistent DNMT3B enrichment. Another possibility is SIRT1-mediated increase in binding affinity of PRC4 polycomb complex that was shown to contain DNMT3B [82–84]. SIRT1 associates with polycomb proteins in PRC4 [82], which may subsequently recruit DNMT3B [83]. Considering the capability of SIRT1 to modify the activity of non-histone proteins through deacetylation, as demonstrated for numerous transcription factors and coregulators [85], it is probable that SIRT1 regulates the activity of a transcriptional repressor that interacts with DNMT3B. Indeed, DNMT3B recruitment was dependent on binding of E2F6 transcriptional repressor in somatic tissues in a mouse model [86,87].

Our findings provide evidence for SIRT1-dependent epigenetic downregulation of *rDNA* and thus potential reduction in ribosomal biogenesis in response to GEN (Figure 5). When *SIRT1* is depleted, GEN no longer leads to suppression of *rDNA* at mRNA levels. To our knowledge, our current study delivers the first evidence that mechanistically connects SIRT1 to *rDNA* transcriptional activity upon GEN treatment. SIRT1-mediated action of GEN has been previously reported, however, without identifying gene targets or mechanisms [28,29]. GEN mitigated acetaminophen-induced liver toxicity by upregulating SIRT1 protein expression and this protective effect was abolished by SIRT1 knockdown [28]. In mice with induced renal injury, the protective effects of GEN were eliminated after stable knockdown of SIRT1 [29]. Furthermore, no previous reports have assessed a direct regulatory action of SIRT1 and SIRT1-DNMT3B interplay on *rDNA* transcriptional activity. Existing studies on human normal and cancer cells of different origins report on the energy-dependent nucleolar silencing complex (eNoSC) which contains SIRT1, among other proteins, and downregulates rRNA transcription upon reduction of energy status [88,89]. In another study on human cells, depletion of AROS, an active regulator of SIRT1 that binds to and upregulates SIRT1, led to impaired ribosomal biogenesis and reduced ribosomal proteins [90]. However, no mechanistic connection to SIRT1 was investigated.

As for *RNF169*, we still observed *RNF169* downregulation in response to GEN when *SIRT1* was depleted (Figure 5(c)). We propose this might be due to the roles of other members from the sirtuin family, which could potentially take over SIRT1 roles. Similar to SIRT1, SIRT6 and SIRT7 are

nuclear sirtuins that exert epigenetic influence on gene expression through the deacetylase activity [91,92]. Furthermore, both SIRT6 and SIRT7 act as a DNA damage sensor and enhance DNA repair [91,92]. Therefore, as the function of *RNF169* is associated with DNA repair (Table 1), there is a likelihood that either SIRT6 or SIRT7 mediates downregulation of *RNF169* when SIRT1 is missing. However, whether GEN acts through SIRT6 and/or SIRT7 remains to be elucidated.

An interesting point to consider is whether SIRT1 or DNMT3B could constitute direct targets of phytoestrogen regulation. Our published work on polyphenols, specifically PTS, indicate that the epigenetic mechanisms are required for the compounds to exert their action on transcriptional gene regulation. We have previously shown that knockout of DNMT3B using CRISPR-Cas9 abolishes effects of PTS on silencing of oncogenes in breast cancer cells [38]. The compounds most probably work through the initiation of intracellular signaling, e.g., via their ROS scavenging activity or upregulating the receptor and signaling cascades of communication between cells. Nevertheless, polyphenols were shown to penetrate through the plasma membrane into the cytoplasm where they interact with proteins, lipids and polynucleotides through electrostatic, hydrophobic, and covalent binding [93]. Polyphenols have been shown to potentially enter all cell compartments [94]. Hence, their interaction with epigenetic enzymes inside the cell could be possible and warrants further investigations.

In conclusion, our findings deliver new evidence for distinct mechanisms of the epigenetic action of PTS and GEN in regulation of gene transcription in human mammary epithelial cells. We showed that only GEN treatment led to the enrichment of DNMT3B within SIRT1-occupied regions at the hypermethylated promoters of *RNF169* and *rDNA*. Although PTS downregulated *RNF169* and *rDNA* expression, it led to SIRT1 enrichment only within *RNF169* promoter and to DNA hypermethylation only within *rDNA* promoter, with no detectable binding of DNMT3B. These breakthrough findings indicate that PTS exerts its epigenetic effects through an alternative mechanism, which remains to be explored in future research. Thus, our novel discovery opens the door to further investigations in the nutritional epigenomics field. Additionally, by elucidating the involvement of SIRT1/DNMT3B in regulating the expression of key genes such as *rDNA* and *RNF169*, roles of which are crucial for health maintenance, longevity and homeostasis, our study offers valuable insights into potential beneficial effects of phytoestrogens in preserving cellular health. This new knowledge may facilitate the application of epigenetic interventions for health maintenance, which is especially important given the aging global population and the rising prevalence of age-related diseases.

Disclosure statement

No potential conflict of interest was reported by the author(s).

Funding

This research was supported by the Natural Sciences and Engineering Research Council (NSERC) Discovery Grant [RGPIN-2021-02969] and Discovery Launch Supplement [DGECR-2021-00286], as well as the Canada Foundation for Innovation John R. Evans Leadership Fund and BC Knowledge Development Fund [#37105], granted to B.S.

Data availability statement

The Authors will share the data upon request. Genome-wide data is available under GEO accession number GSE113299 (DNA methylation microarray-in vitro model) and GSE278528 (RNA sequencing-in vivo model).

ORCID

Barbara Stefanska http://orcid.org/0000-0002-1186-3210

References

[1] Nishiyama A, Nakanishi M. Navigating the DNA methylation landscape of cancer. Trends Genet. 2021;37(11):1012–1027. doi: 10.1016/j.tig.2021.05.002

[2] Wang K, Liu H, Hu Q, et al. Epigenetic regulation of aging: implications for interventions of aging and diseases. Sig Transduct Target Ther. 2022;7(1):374. doi: 10.1038/s41392-022-01211-8

[3] de Mendoza A, Nguyen TV, Ford E, et al. Large-scale manipulation of promoter DNA methylation reveals context-specific transcriptional responses and stability.

Genome Biol. 2022;23(1):163. doi: 10.1186/s13059-022-02728-5

[4] Cedar H, Bergman Y. Linking DNA methylation and histone modification: patterns and paradigms. Nat Rev Genet. 2009;10(5):295–304. doi: 10.1038/nrg2540

[5] Rose NR, Klose RJ. Understanding the relationship between DNA methylation and histone lysine methylation. Biochim Et Biophys Acta (BBA) - Gene Regul Mechanisms. 2014;1839(12):1362–1372. doi: 10.1016/j.bbagrm.2014.02.007

[6] Li Y, Chen X, Lu C. The interplay between DNA and histone methylation: molecular mechanisms and disease implications. EMBO Rep. 2021;22(5):e51803. doi: 10.15252/embr.202051803

[7] Li T, Garcia-Gomez A, Morante-Palacios O, et al. SIRT1/2 orchestrate acquisition of DNA methylation and loss of histone H3 activating marks to prevent premature activation of inflammatory genes in macrophages. Nucleic Acids Res. 2020;48(2):665–681. doi: 10.1093/nar/gkz1127

[8] Kashiwagi K, Nimura K, Ura K, et al. DNA methyltransferase 3b preferentially associates with condensed chromatin. Nucleic Acids Res. 2011;39(3):874–888. doi: 10.1093/nar/gkq870

[9] Lee MK, Kim T. Histone H4-specific deacetylation at active coding regions by Hda1C. Mol Cells. 2020;43(10):841–847. doi: 10.14348/molcells.2020.0141

[10] O'Hagan HM, Mohammad HP, Baylin SB, et al. Double strand breaks can initiate gene silencing and SIRT1-dependent onset of DNA methylation in an exogenous promoter CpG island. PLOS Genet. 2008;4(8):e1000155. doi: 10.1371/journal.pgen.1000155

[11] Wu Q-J, Zhang T-N, Chen H-H, et al. The sirtuin family in health and disease. Sig Transduct Target Ther. 2022;7(1):402. doi: 10.1038/s41392-022-01257-8

[12] Peng L, Yuan Z, Ling H, et al. SIRT1 deacetylates the DNA methyltransferase 1 (DNMT1) protein and alters its activities. Mol Cell Biol. 2011;31(23):4720–4734. doi: 10.1128/MCB.06147-11

[13] Brunet A, Sweeney LB, Sturgill JF, et al. Stress-dependent regulation of FOXO transcription factors by the SIRT1 deacetylase. Science. 2004;303(5666):2011–2015. doi: 10.1126/science.1094637

[14] Kauppinen A, Suuronen T, Ojala J, et al. Antagonistic crosstalk between nf-κB and SIRT1 in the regulation of inflammation and metabolic disorders. Cell Signal. 2013;25(10):1939–1948. doi: 10.1016/j.cellsig.2013.06.007

[15] Rodgers JT, Lerin C, Haas W, et al. Nutrient control of glucose homeostasis through a complex of PGC-1α and SIRT1. Nature. 2005;434(7029):113–118. doi: 10.1038/nature03354

[16] Liu Z, Liu H, Liu S, et al. SIRT1 activation promotes bone repair by enhancing the coupling of type H vessel formation and osteogenesis. Cell Prolif. 2024;57(6):e13596. doi: 10.1111/cpr.13596

[17] Iside C, Scafuro M, Nebbioso A, et al. SIRT1 activation by natural phytochemicals: an overview. Front Pharmacol. 2020;11:1225. doi: 10.3389/fphar.2020.01225

[18] Beetch M, Harandi-Zadeh S, Shen K, et al. Dietary antioxidants remodel DNA methylation patterns in chronic disease. Br J Pharmacol. 2020;177(6):1382–1408. doi: 10.1111/bph.14888

[19] Borra MT, Smith BC, Denu JM. Mechanism of human SIRT1 activation by resveratrol. J Biol Chem. 2005;280(17):17187–17195. doi: 10.1074/jbc.M501250200

[20] Pacholec M, Bleasdale JE, Chrunyk B, et al. SRT1720, SRT2183, SRT1460, and resveratrol are not direct activators of SIRT1. J Biol Chem. 2010;285(11):8340–8351. doi: 10.1074/jbc.M109.088682

[21] Kala R, Shah HN, Martin SL, et al. Epigenetic-based combinatorial resveratrol and pterostilbene alters DNA damage response by affecting SIRT1 and DNMT enzyme expression, including SIRT1-dependent γ-H2AX and telomerase regulation in triple-negative breast cancer. BMC Cancer. 2015;15(1):672. doi: 10.1186/s12885-015-1693-z

[22] Wang P, Sang S. Metabolism and pharmacokinetics of resveratrol and pterostilbene. Biofactors. 2018;44(1):16–25. doi: 10.1002/biof.1410

[23] Liu D, Ma Z, Xu L, et al. PGC1α activation by pterostilbene ameliorates acute doxorubicin cardiotoxicity by reducing oxidative stress via enhancing AMPK and SIRT1 cascades. Aging (Albany NY). 2019;11(22):10061–10073. doi: 10.18632/aging.102418

[24] Koh YC, Lin SJ, Hsu KY, et al. Pterostilbene enhances thermogenesis and mitochondrial biogenesis by activating the SIRT1/PGC-1α/SIRT3 pathway to prevent Western diet-induced obesity. Mol Nutr Food Res. 2023;67(18):e2300370. doi: 10.1002/mnfr.202300370

[25] Zhu L, Lu F, Zhang X, et al. SIRT1 is involved in the neuroprotection of pterostilbene against amyloid β 25–35-Induced cognitive deficits in mice. Front Pharmacol. 2022;13:877098. doi: 10.3389/fphar.2022.877098

[26] Zhu Q, Tang T, Liu H, et al. Pterostilbene attenuates cocultured BV-2 microglial inflammation-mediated SH-SY5Y neuronal oxidative injury via SIRT-1 signalling. Oxid Med Cell Longev. 2020;2020:1–11. doi: 10.1155/2020/3986348

[27] Jiang Z, Wang H, Yang Y, et al. Genistein activated SIRT1-AMPK signaling pathway mediated by ERβ-FOXO1-Nampt to reduce fat accumulation in chicken hepatocytes. Life Sci. 2023;312:121259. doi: 10.1016/j.lfs.2022.121259

[28] Wang L, Li A, Liu Y, et al. Genistein protects against acetaminophen-induced liver toxicity through augmentation of SIRT1 with induction of Nrf2 signalling. Biochem Biophys Res Commun. 2020;527(1):90–97. doi: 10.1016/j.bbrc.2020.04.100

[29] Li WF, Yang K, Zhu P, et al. Genistein ameliorates ischemia/reperfusion-induced renal injury in a

SIRT1-dependent manner. Nutrients. 2017;9(4):403. doi: 10.3390/nu9040403

[30] Zhou C, Li D, Ding C, et al. Involvement of SIRT1 in amelioration of schistosomiasis-induced hepatic fibrosis by genistein. Acta Trop. 2021;220:105961. doi: 10.1016/j.actatropica.2021.105961

[31] Beetch M, Lubecka K, Shen K, et al. Stilbenoid-mediated epigenetic activation of semaphorin 3A in breast cancer cells involves changes in dynamic interactions of DNA with DNMT3A and NF1C transcription factor. Mol Nutr Food Res. 2019;63(19):e1801386. doi: 10.1002/mnfr.201801386

[32] Kala R, Tollefsbol TO, Castresana JS. A novel combinatorial epigenetic therapy using resveratrol and pterostilbene for restoring estrogen receptor-α (ERα) expression in ERα-negative breast cancer cells. PLOS ONE. 2016;11(5):e0155057. doi: 10.1371/journal.pone.0155057

[33] Bilir B, Sharma NV, Lee J, et al. Effects of genistein supplementation on genome-wide DNA methylation and gene expression in patients with localized prostate cancer. Int J Oncol. 2017;51(1):223–234. doi: 10.3892/ijo.2017.4017

[34] Majid S, Dar AA, Shahryari V, et al. Genistein reverses hypermethylation and induces active histone modifications in tumor suppressor gene B-Cell translocation gene 3 in prostate cancer. Cancer. 2010;116(1):66–76. doi: 10.1002/cncr.24662

[35] Sundaram MK, Unni S, Somvanshi P, et al. Genistein modulates signaling pathways and targets several epigenetic markers in HeLa cells. Genes (Basel). 2019;10(12):10. doi: 10.3390/genes10120955

[36] Donovan MG, Selmin OI, Doetschman TC, et al. Epigenetic activation of BRCA1 by genistein in vivo and triple negative breast cancer cells linked to antagonism toward aryl hydrocarbon receptor. Nutrients. 2019;11(11):11. doi: 10.3390/nu11112559

[37] Xie Q, Bai Q, Zou LY, et al. Genistein inhibits DNA methylation and increases expression of tumor suppressor genes in human breast cancer cells. Genes Chromosomes Cancer. 2014;53(5):422–431. doi: 10.1002/gcc.22154

[38] Beetch M, Boycott C, Harandi-Zadeh S, et al. Pterostilbene leads to DNMT3B-mediated DNA methylation and silencing of OCT1-targeted oncogenes in breast cancer cells. J Nutr Biochem. 2021;98:108815. doi: 10.1016/j.jnutbio.2021.108815

[39] Harandi-Zadeh S, Boycott C, Beetch M, et al. Pterostilbene changes epigenetic marks at enhancer regions of oncogenes in breast cancer cells. Antioxidants (Basel). 2021;10(8):10. doi: 10.3390/antiox10081232

[40] Sharma M, Arora I, Chen M, et al. Therapeutic effects of dietary soybean genistein on triple-negative breast cancer via regulation of epigenetic mechanisms. Nutrients. 2021;13(11):3944. doi: 10.3390/nu13113944

[41] Beetch M, Lubecka K, Kristofzski H, et al. Subtle alterations in DNA methylation patterns in normal cells in response to dietary stilbenoids. Mol Nutr Food Res. 2018;62(14):e1800193. doi: 10.1002/mnfr.201800193

[42] Gross SM, Dane MA, Smith RL, et al. A multi-omic analysis of MCF10A cells provides a resource for integrative assessment of ligand-mediated molecular and phenotypic responses. Commun Biol. 2022;5(1):1066. doi: 10.1038/s42003-022-03975-9

[43] Puleo J, Polyak K. The mCF10 model of breast tumor progression. Cancer Res. 2021;81(16):4183–4185. doi: 10.1158/0008-5472.CAN-21-1939

[44] Schmittgen TD, Livak KJ. Analyzing real-time PCR data by the comparative CT method. Nat Protoc. 2008;3(6):1101–1108. doi: 10.1038/nprot.2008.73

[45] Boycott C, Beetch M, Yang T, et al. Epigenetic aberrations of gene expression in a rat model of hepatocellular carcinoma. Epigenet. 2022;17(11):1513–1534. doi: 10.1080/15592294.2022.2069386

[46] Peng GH, Chen S. Double chromatin immunoprecipitation: analysis of target co-occupancy of retinal transcription factors. Methods Mol Biol. 2013;935:311–328.

[47] Barrett T, Wilhite SE, Ledoux P, et al. NCBI GEO: archive for functional genomics data sets—update. Nucleic Acids Res. 2013;41(D1):D991–5. doi: 10.1093/nar/gks1193

[48] Park SJ, Yoon BH, Kim SK, et al. GENT2: an updated gene expression database for normal and tumor tissues. BMC Med Genomics. 2019;12(S5):101. doi: 10.1186/s12920-019-0514-7

[49] Chelius X, Bartosch V, Rausch N, et al. Selective retention of dysfunctional mitochondria during asymmetric cell division in yeast. PLOS Biol. 2023;21(9):e3002310. doi: 10.1371/journal.pbio.3002310

[50] Matlashov ME, Belousov VV, Enikolopov G. How much H 2 O 2 is produced by recombinant d-amino acid oxidase in mammalian cells? Antioxid Redox Signal. 2014;20(7):1039–1044. doi: 10.1089/ars.2013.5618

[51] Lin A, Hokugo A, Choi J, et al. Small cytoskeleton-associated molecule, fibroblast growth factor receptor 1 oncogene partner 2/wound inducible transcript-3.0 (FGFR1OP2/wit3.0), facilitates fibroblast-driven wound closure. Am J Pathol. 2010;176(1):108–121. doi: 10.2353/ajpath.2010.090256

[52] Caley MP, Martins VL, O'Toole EA. Metalloproteinases and wound healing. Adv Wound Care (New Rochelle). 2015;4(4):225–234. doi: 10.1089/wound.2014.0581

[53] Toriseva M, Laato M, Carpen O, et al. MMP-13 regulates growth of wound granulation tissue and modulates gene expression signatures involved in inflammation, proteolysis, and cell viability. PLOS ONE. 2012;7(8):e42596. doi: 10.1371/journal.pone.0042596

[54] Lei X, Du L, Yu W, et al. GSTP1 as a novel target in radiation induced lung injury. J Transl Med. 2021;19(1):297. doi: 10.1186/s12967-021-02978-0

[55] Ferrer CM, Cho HM, Boon R, et al. The glutathione S-transferase Gstt1 drives survival and dissemination in metastases. Nat Cell Biol. 2024;26(6):975–990. doi: 10.1038/s41556-024-01426-7

[56] Qian J, Song Z, Lv Y, et al. Glutathione S-Transferase T1 null genotype is associated with susceptibility to inflammatory bowel disease. Cell Physiol Biochem. 2017;41(6):2545–2552. doi: 10.1159/000475978

[57] Tacho-Pinot R, Stamper CT, King JI, et al. Bcl6 is a subset-defining transcription factor of lymphoid tissue inducer-like ILC3. Cell Rep. 2023;42(11):113425. doi: 10.1016/j.celrep.2023.113425

[58] Kubo S, Kataria R, Yao Y, et al. Early B cell factor 4 modulates fas-mediated apoptosis and promotes cytotoxic function in human immune cells. Proc Natl Acad Sci USA. 2022;119(33):e2208522119. doi: 10.1073/pnas.2208522119

[59] Poulsen M, Lukas C, Lukas J, et al. Human RNF169 is a negative regulator of the ubiquitin-dependent response to DNA double-strand breaks. J Cell Biol. 2012;197(2):189–199. doi: 10.1083/jcb.201109100

[60] Longarini EJ, Dauben H, Locatelli C, et al. Modular antibodies reveal DNA damage-induced mono-adp-ribosylation as a second wave of PARP1 signaling. Mol Cell. 2023;83(10):1743–1760.e11. doi: 10.1016/j.molcel.2023.03.027

[61] Rodriguez MS, Egaña I, Lopitz-Otsoa F, et al. The RING ubiquitin E3 RNF114 interacts with A20 and modulates nf-κB activity and T-cell activation. Cell Death Dis. 2014;5(8):e1399–e. doi: 10.1038/cddis.2014.366

[62] Bijlmakers MJ, Kanneganti SK, Barker JN, et al. Functional analysis of the RNF114 psoriasis susceptibility gene implicates innate immune responses to double-stranded RNA in disease pathogenesis. Hum Mol Genet. 2011;20(16):3129–3137. doi: 10.1093/hmg/ddr215

[63] Kuang E, Okumura CY, Sheffy-Levin S, et al. Regulation of ATG4B stability by RNF5 limits basal levels of autophagy and influences susceptibility to bacterial infection. PLOS Genet. 2012;8(10):e1003007. doi: 10.1371/journal.pgen.1003007

[64] MacInnes AW. The role of the ribosome in the regulation of longevity and lifespan extension. Wiley Interdiscip Rev RNA. 2016;7(2):198–212. doi: 10.1002/wrna.1325

[65] Jiao L, Liu Y, Yu XY, et al. Ribosome biogenesis in disease: new players and therapeutic targets. Sig Transduct Target Ther. 2023;8(1):15. doi: 10.1038/s41392-022-01285-4

[66] Buchwalter A, Hetzer MW. Nucleolar expansion and elevated protein translation in premature aging. Nat Commun. 2017;8(1):328. doi: 10.1038/s41467-017-00322-z

[67] Pelletier J, Thomas G, Volarevic S. Ribosome biogenesis in cancer: new players and therapeutic avenues. Nat Rev Cancer. 2018;18(1):51–63. doi: 10.1038/nrc.2017.104

[68] Kovalski JR, Kuzuoglu-Ozturk D, Ruggero D. Protein synthesis control in cancer: selectivity and therapeutic targeting. Embo J. 2022;41(8):e109823. doi: 10.15252/embj.2021109823

[69] Santolla MF, Avino S, Pellegrino M, et al. SIRT1 is involved in oncogenic signaling mediated by GPER in breast cancer. Cell Death Dis. 2015;6(7):e1834. doi: 10.1038/cddis.2015.201

[70] Khan M, Ullah R, Rehman SU, et al. 17β-estradiol modulates SIRT1 and halts oxidative stress-mediated cognitive impairment in a male aging mouse model. Cells. 2019;8(8):928. doi: 10.3390/cells8080928

[71] Scaling AL, Prossnitz ER, Hathaway HJ. GPER mediates estrogen-induced signaling and proliferation in human breast epithelial cells and normal and malignant breast. Horm Cancer. 2014;5(3):146–160. doi: 10.1007/s12672-014-0174-1

[72] Wesierska-Gadek J, Schreiner T, Maurer M, et al. Phenol red in the culture medium strongly affects the susceptibility of human MCF-7 cells to roscovitine. Cell Mol Biol Lett. 2007;12(2):280–293. doi: 10.2478/s11658-007-0002-5

[73] Berthois Y, Katzenellenbogen JA, Katzenellenbogen BS. Phenol red in tissue culture media is a weak estrogen: implications concerning the study of estrogen-responsive cells in culture. Proc Natl Acad Sci USA. 1986;83(8):2496–2500. doi: 10.1073/pnas.83.8.2496

[74] Revollo JR, Li X. The ways and means that fine tune Sirt1 activity. Trends Biochem Sci. 2013;38(3):160–167. doi: 10.1016/j.tibs.2012.12.004

[75] Swatek KN, Komander D. Ubiquitin modifications. Cell Res. 2016;26(4):399–422. doi: 10.1038/cr.2016.39

[76] Abdelmohsen K, Pullmann R Jr., Lal A, et al. Phosphorylation of HuR by Chk2 regulates SIRT1 expression. Mol Cell. 2007;25(4):543–557. doi: 10.1016/j.molcel.2007.01.011

[77] Matsumura Y, Wei F-Y, Sakai J. Epitranscriptomics in metabolic disease. Nat Metab. 2023;5(3):370–384. doi: 10.1038/s42255-023-00764-4

[78] Chen J, Deng LL, Xiao XL, et al. An association between decreased small intestinal RNA modification and disturbed glucagon-like peptide-1 secretion under high-fat diet stress. Nutrients. 2023;15(17):15. doi: 10.3390/nu15173707

[79] Ning Y, Chen J, Shi Y, et al. Genistein ameliorates renal fibrosis through regulation snail via m6A RNA demethylase ALKBH5. Front Pharmacol. 2020;11:579265. doi: 10.3389/fphar.2020.579265

[80] Rolicka A, Guo Y, Ganez Zapater A, et al. The chromatin-remodeling complexes B-WICH and NuRD regulate ribosomal transcription in response to glucose. FASEB J. 2020;34(8):10818–10834. doi: 10.1096/fj.202000411R

[81] Koestler SA, Ball ML, Muresan L, et al. Transcriptionally active chromatin loops contain both 'active' and 'inactive' histone modifications that exhibit exclusivity at the level of nucleosome clusters. Epigenet Chromatin. 2024;17(1):8. doi: 10.1186/s13072-024-00535-9

[82] Kuzmichev A, Margueron R, Vaquero A, et al. Composition and histone substrates of polycomb repressive group complexes change during cellular differentiation. Proc Natl Acad Sci USA. 2005;102(6):1859–1864. doi: 10.1073/pnas.0409875102

[83] O'Hagan HM, Wang W, Sen S, et al. Oxidative damage targets complexes containing DNA methyltransferases, SIRT1, and polycomb members to promoter CpG islands. Cancer Cell. 2011;20(5):606–619. doi: 10.1016/j.ccr.2011.09.012

[84] Wakeling LA, Ions LJ, Escolme SM, et al. SIRT1 affects DNA methylation of polycomb group protein target genes, a hotspot of the epigenetic shift observed in ageing. Hum Genomics. 2015;9(1):14. doi: 10.1186/s40246-015-0036-0

[85] Zhang T, Kraus WL. SIRT1-dependent regulation of chromatin and transcription: linking NAD(+) metabolism and signaling to the control of cellular functions. Biochim Biophys Acta. 2010;1804(8):1666–1675. doi: 10.1016/j.bbapap.2009.10.022

[86] Velasco G, Hubé F, Rollin J, et al. Dnmt3b recruitment through E2F6 transcriptional repressor mediates germ-line gene silencing in murine somatic tissues. Proc Natl Acad Sci USA. 2010;107(20):9281–9286. doi: 10.1073/pnas.1000473107

[87] Yang Y, Liu Y, Wang Y, et al. Regulation of SIRT1 and its roles in inflammation. Front Immunol. 2022;13:831168. doi: 10.3389/fimmu.2022.831168

[88] Murayama A, Ohmori K, Fujimura A, et al. Epigenetic control of rDNA loci in response to intracellular energy status. Cell. 2008;133(4):627–639. doi: 10.1016/j.cell.2008.03.030

[89] Yang L, Song T, Chen L, et al. Regulation of SirT1-nucleomethylin binding by rRNA coordinates ribosome biogenesis with nutrient availability. Mol Cell Biol. 2013;33(19):3835–3848. doi: 10.1128/MCB.00476-13

[90] Knight JR, Willis AE, Milner J. Active regulator of SIRT1 is required for ribosome biogenesis and function. Nucleic Acids Res. 2013;41(7):4185–4197. doi: 10.1093/nar/gkt129

[91] Onn L, Portillo M, Ilic S, et al. SIRT6 is a DNA double-strand break sensor. Elife. 2020;9. doi: 10.7554/eLife.51636

[92] Vazquez BN, Thackray JK, Simonet NG, et al. SIRT7 promotes genome integrity and modulates non-homologous end joining DNA repair. Embo J. 2016;35(14):1488–1503. doi: 10.15252/embj.201593499

[93] Lewandowska H, Kalinowska M, Lewandowski W, et al. The role of natural polyphenols in cell signaling and cytoprotection against cancer development. J Nutr Biochem. 2016;32:1–19. doi: 10.1016/j.jnutbio.2015.11.006

[94] Lorenz M. Cellular targets for the beneficial actions of tea polyphenols. Am J Clin Nutr. 2013;98(6):1642S–1650S. doi: 10.3945/ajcn.113.058230